

Symbolic description of 3-D structures applied to cerebral vessel tree obtained from MR angiography volume data

G. Gerig, Th. Koller, G. Székely, Ch. Brechbühler and O. Kübler

Communication Technology Laboratory, Image Science,
ETH-Zentrum, CH-8092 Zurich, Switzerland
e-mail: gerig@vision.ethz.ch

The present paper focuses on the conversion of multidimensional image structures to an object-centered, abstract description encoding shape features and structure relationships. We describe a prototype system that extracts three-dimensional (3-D) curvilinear structures from volume image data and transforms them into a symbolic description which represents topological and geometrical features of tree-like, filamentous objects.

The initial segmentation is performed by 3-D hysteresis thresholding. A skeletal structure is derived by 3-D binary thinning, approximating the center-lines while fully preserving the 3-D topology. The local width of the line structures is characterized by a separate 3-D Euclidean distance transform. Compilation, or raster-to-vector transformation, converts the maximally thinned voxel lists into a vector description. The final graph data-structure encodes the spatial course of line sections, the estimate of the local diameter, and the topology at important key locations like branchings and end-points.

The analysis system is applied to the characterization of the cerebral vascular system segmented from magnetic resonance angiography (MRA).

Keywords: Multidimensional image analysis, 3-D binary thinning, 3-D raster-to-vector transform, symbolic representation, magnetic resonance angiography, cerebrospinal vasculature

1 Introduction & Motivation

The value of computer assisted systems for presentation, manipulation and quantitation of objects obtained from multidimensional image data depends critically on the ability to segment and also describe structures in images. Although segmentation is still considered as a most crucial step in image analysis, this paper draws the attention to a topic less often described, namely to the symbolic description of image structures.

The development of the prototype system is driven by the application of assessing the cerebral vascular tree in magnetic resonance (MR) volume data. Illustrations of intermediate results will guide the discussion of the processing steps. The special MR angiography (MRA) technique suppresses or eliminates signal from stationary tissue and enhances the appearance of flow, providing high

contrast between flowing blood and surrounding soft tissue. Therefore, blood-vessels in volume data are represented as filamentous, curvilinear structures with high intensities.

The MRA acquisition technology has improved a lot during the last years and offers rapid, noninvasive 3-D mapping of the vascular structures. The evaluation of vascular information, however, is severely limited by the lack of appropriate computerized analysis tools regarding visualization and description of structures:

- **Visualization:** Nowadays, MRA data are most often presented by two-dimensional maximum intensity projection (MIP), with its inherent shortcomings of obscuring features and creating irregular depth cues [1, 2, 3]. The MIP technique displays the maximum voxel value encountered along each ray cast into the volume. It favors the demonstration of high intensities along projection rays over finer structures even when they are located nearer to the observer, obscuring features and creating irregular depth cues. A limited 3-D impression is obtained only from cine-mode displays or stereoscopic views. Several groups approached the problem of poor visualization by augmenting the MIP technique with information about vessel width, depth and connectivity [4, 3]. Others demonstrated integrated displays of anatomical surfaces segmented from MRI and maximum intensity projections of MRA data [1, 5, 2].

Three-dimensional rendering of the *segmented vascular tree* represents an alternative visualization approach. Although the segmentation of fine vessels (down to one voxel size) still needs improvement, the 3-D rendering of the larger vessels could clearly demonstrate its advantage over maximum intensity projection [6, 7].

- **Structure description:** Successful segmentation of volume data into anatomically and functionally meaningful objects and tissue categories has created new possibilities for 3-D planning, intervention and for quantitative volumetric studies, but it doesn't provide any information characterizing the gross form or some detailed shape features answering particular clinical questions regarding vessel morphology and local flow information.

Therapy and planning require more information than simply the presence of diseases, since the *medical task being the measurement* of vessel diameters, distances, and shapes or the identification of the topology of structures. The clinical task of analyzing image data includes *structure* and *shape* as important descriptive features. A structural analysis and comparison of image information goes beyond a segmentation into constituent components and requires new methods for the description of image structures.

Offering access to geometrical and topological properties, the binary array representation of the segmented vascular tree has to be transformed into a more appropriate data structure. Volumetric primitives of tubular structures strongly

resemble the model of “generalized cylinders” with circular cross-section, suggesting the appropriateness of a skeleton or medial axis description (MAT [8]). Further, the biological variability of the vasculature favors a *description based on topological features* rather than on exact geometry. While a voxel to voxel registration of the blood vessel pattern among different patients or between patient data and an anatomical atlas data seems to be unrealistic due to individual variations, one can think of coding the topological variations [9]. Typical examples of topological relations are “is continuation of” and “adjoins to”. Expressions like “circulus arteriosus cerebri” for the central blood vessel circle or “arteria communicans post.” suggest the use of topological shape criteria. A topological description based on a skeleton structure would also meet the requirement for invariance, capability of dealing with variable appearance and representation in terms of perceivable shapes.

2 Segmentation and description of 3-D lines

2.1 Segmentation by hysteresis thresholding

The special MRA acquisition technique simplifies the segmentation of large vessels by producing high contrast for vascular structures. A binarization technique suffices to segment the major vessels. However, small vessels with diameters of one voxel ($\approx 1\text{mm}$) and smaller are subject to partial voluming and noise fluctuations. If the selected threshold is high, many of the voxels belonging actually to the object to be segmented will get lost. On the other hand a low threshold value leads to the inclusion of many noise voxels, impeding the subsequent topological analysis considerably. Similar problems with binarization of the matched filter output in an edge detection method led to the development of a hysteresis thresholding procedure [10, 11].

Hysteresis thresholding works simultaneously with two threshold values. The upper threshold identifies a certainty level above which a voxel most probably belongs to the structure of interest. Consequently those voxels will be part of the resulting segment and act as seed regions. The lower threshold specifies the noise level below which voxels will be excluded. Voxels with intensities between the lower and upper threshold will be only selected if they are connected to a seed region.

As the cerebral vessel tree is by definition a connected segment, it seems to be reasonable to adopt the hysteresis thresholding strategy to the raw MRA data. The 3-D application of this technique to detect connected edge-surfaces has been already previously investigated [12]. Our experience showed that the application of double thresholding for 3-D edge (surface) detection did not significantly differ from simple thresholding. The reason for this surprising behavior is the high connectivity of surface fragments in 3-D space. In the case of vessel tree segmentation, however, the structure we are looking for is composed of thin lines with a very sparse space occupation, reducing the number of random connections. Figure 1 illustrates the effective noise reduction by hysteresis thresholding.

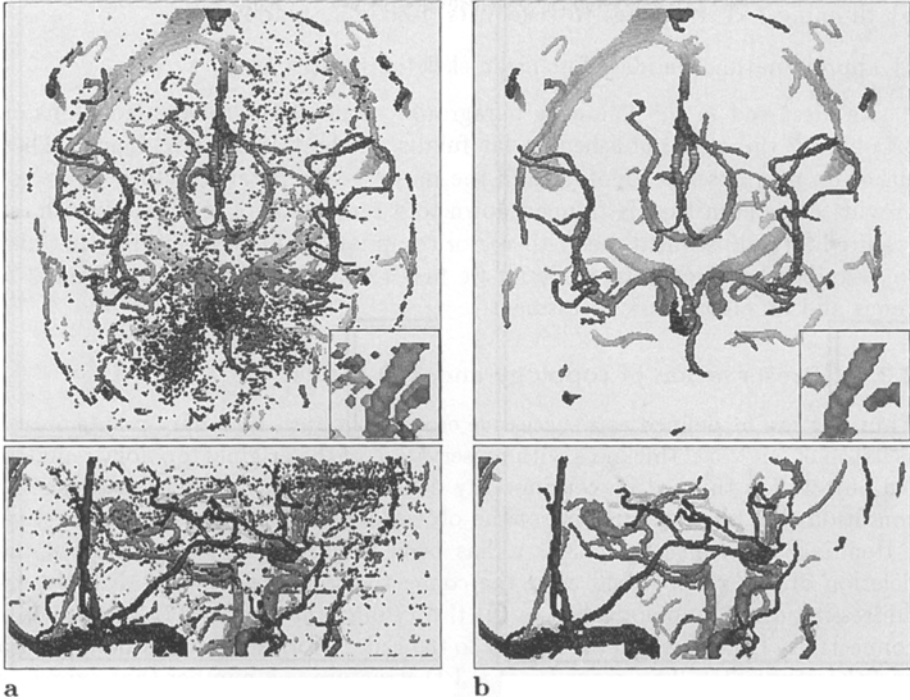


Figure 1: Three-dimensional rendering of the segmented vessel tree (top view): a) simple thresholding, b) hysteresis thresholding. The lower threshold in b corresponds to the single threshold used in Figure a, it corresponds to 50% of the higher threshold generating the seed regions. The small Figures represent zoomed regions (250%)

2.2 3-D binary thinning

Blum's classical proposal [8] presented the description of shapes in 2-D binary images by the medial axis transformation (MAT). The MAT generates an object-centered, invariant description of shapes in terms of their medial axis. Additionally, the technique decomposes structures and sub-structures by generating a tree-like representation. Early implementations of skeletonization procedures in 2-D have focussed on erosion by preserving topology (thinning: [13, 14]) or on metric properties (finding relative maxima in distance transforms: [15, 16]). Similarly, an approximative skeleton of binary volumes can be obtained by extending these approaches to 3-D. Herein, binary thinning was chosen for the generation of topologically correct skeletons for filamentous tree-like structures, considering that the preservation of topology offered by these techniques is more important than a perfect medialness.

A 3-D thinning algorithm was implemented based on three requirements:

a) preserving topology,

- b) thinning 3-D structures to voxel lists (maximal thinning), and
- c) approximating the ideal Euclidean skeleton (center line).

As discussed in the following paragraphs, none of the many algorithms on 3-D binary thinning published so far fulfills all the three requirements. They either do not preserve topology and the major geometrical structure or do not provide a skeleton that is thinned down to a center-line of one voxel width, as required for a subsequent raster-to-vector compilation of line structures. In order to describe the algorithms in detail we first reconsider the concept of the 3-D genus and its algorithmic assessment.

2.2.1 Preservation of topology and 3-D genus

Thinning can be defined as a successive erosion of object boundary points until a skeleton of one voxel thickness with preservation of the original topology remains. An object S is thinned by continuously deleting boundary voxels based on the condition that the connectivity of the object and its complement is preserved. Extending 2-D concepts to 3-D it has been proposed to check locally if the deletion of one voxel would alter the connectivity of the object. Most papers addressing digital topology discuss the theory of simple points [17, 18] or surface connectivity [19, 20] which are related to the Euler's formula for closed polyhedra and the genus [21]. The genus χ_3 of a 3-D structure is a number that expresses global topological properties,

$$\chi_3(S) = \text{Objects}(S) + \text{Cavities}(S) - \text{Holes}(S). \quad (1)$$

The appendix demonstrates how the *global* genus can be calculated using *local* measurements on elements of a connectivity graph, which are vertices, edges, faces and cells. A thinning operation should not delete or separate objects and not fill or create cavities and handles. It can be shown for the 2-D case that *constancy of the genus* χ_2 (number of objects minus number of holes) while removing the center pixel in 3x3 windows preserves the topology, because it is not possible to create a hole and at the same time split an object structure. The 3-D case, however, requires a more careful analysis. As expressed in equation 1, the genus χ_3 can be written as the number of objects plus the number of cavities minus the number of holes. If through the deletion of a voxel either the number of objects, of cavities or of holes changes, the genus will reflect the topological change. However, the creation of objects or cavities while *simultaneously* increasing the number of holes can counteract and result in an unaltered genus. Creating a cavity and an additional hole by deleting the central voxel in a 3x3x3 voxel neighborhood is not possible (no hole can be created if all 6-neighbors are set), but objects can be split while producing a new hole as shown in Figure 2(a). The example consists of a rod on top of a 4-voxel ring. The 3-D genus before and after deletion of the central voxel equals to 1, either representing 1 object or 2 objects and 1 hole. Other cases can be considered where, for example, 2 new objects and 2 new holes can be created.

The result obtained above is not surprising if one considers that the 3-D genus $\chi_3(S)$ as used in the sense of Morgenthaler [21] represents a *topological number of a collection of components* rather than a single component¹. However, it clearly demonstrates that a 3-D thinning algorithm based solely on the constancy of the genus (e.g. [19]) or a straightforward extension of 2-D algorithms does not necessarily preserve the connectivity of structures. While the number of objects and cavities are easy to determine by connected component labeling, the practical value of the 3-D genus may be seen in the fact that it gives control over the number of holes.

2.2.2 Discussion of thinning algorithms

Tsao and Fu [20] proposed a parallel implementation of binary thinning to minimize the execution time. Parallel processing requires a careful consideration of the connectivity constraints because a simultaneous removal of voxels can separate or even eliminate objects. Tsao and Fu divide each thinning iteration into six sub-cycles performing subsequent partial erosions from U,B,N,S,W,E-directions. Connectivity is not only tested in $3 \times 3 \times 3$ neighborhoods but also on 3×3 “checking planes” with normals perpendicular to the active directions. The algorithm results in medial surfaces and can create medial axes by a further thinning with relaxed conditions. Own tests demonstrated that topology is preserved but that the algorithm gives results which are highly sensitive to the orientation of structures and does not provide a maximally thinned skeleton. Figure 2(b) shows a plane with normal (1,1,1) which cannot be thinned to a medial axis due to the preference of structures oriented along the main axes.

Lobregt et al. [19] used the sum of the Euler characteristics of closed surfaces to derive a 3-D thinning algorithm. The approach divided a $3 \times 3 \times 3$ neighborhood into eight $2 \times 2 \times 2$ sub-neighborhoods in order to apply precalculated tables expressing local contributions to the connectivity number. The check if the deletion of one voxel will affect the connectivity of the object is based on the 3-D genus (surface connectivity). The discussion in the previous subsection clearly illustrates that for certain configurations the topology is not preserved.

Bertrand and Malandain [22, 23] proposed a topological classification of voxels based on the number of connected components that guides a pseudo-parallel binary thinning process. The characterization of voxels as interior, isolated, border, curve, surface and junction points allows a selective removal of voxels which are not part of medial surfaces, medial axes or junctions thereof. The algorithm performs iterations with six sub-cycles (U,B,N,S,W,E-directions), where so-called “simple points”, i.e. points that are part of an object boundary or line-ends, exposed to the active direction are removed in parallel. This algorithm correctly detects voxels within the thin surface in Figure 2(b) as points of a medial surface. The surface borders, however, are classified as simple points and are candidates to be deleted in parallel. All the voxels of a medial surface structure with 2 voxel width, as shown in Figure 2(c), are marked as simple

¹The genus of *one* single object is a topological invariant.

points (border points). According to [22], edge points of a simple surface will be deleted at the first cycle. It is not clear from the description in the paper how structures like Fig. 2(c) are preserved from being deleted. Recently, the thinning scheme based on topological classification has been slightly changed by replacing the parallel deletion in each sub-cycle with a sequential thinning of all voxels exposed to the active direction (Malandain, private communication). The configuration shown in Figure 2(a) will be correctly classified as a surface-curve junction.

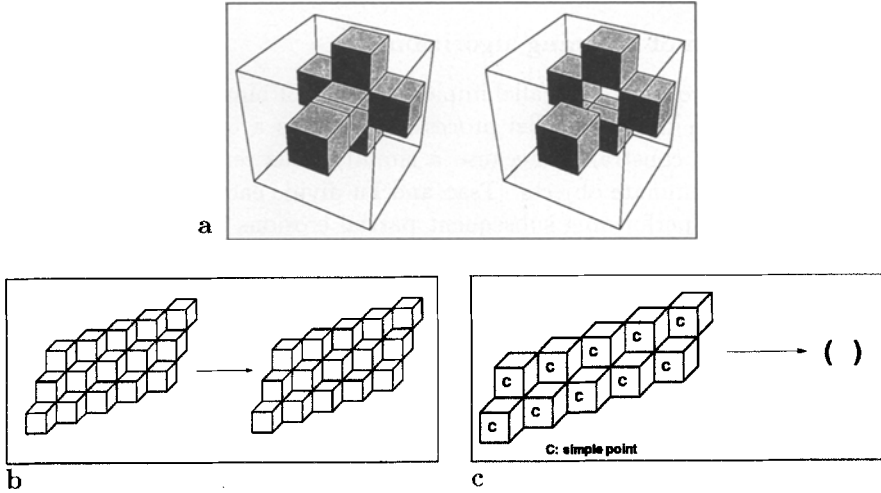


Figure 2: Problems with binary 3-D thinning: a) The preservation of the 3-D genus χ_3 can violate the topology, for example by creating an additional object component and a new hole. b) Parallel thinning as proposed by Tsao and Fu cannot thin surface structures to medial lines if they are not oriented like the planes $x = i$, $y = j$, $z = k$. c) Parallel thinning of simple points resulting from a topological classification (Bertrand and Malandain) can eliminate structures, because every point is a border point and will be deleted simultaneously.

2.2.3 Three-dimensional thinning of structures to medial curves

Based on the requirements stated in subsection 2.2 we implemented a pseudo-parallel binary thinning scheme. The application to tree-like line patterns implies an erosion of structures to medial curves rather than medial surfaces. Unlike Tsao and Fu, the motivation for applying an iterative pseudo-parallel thinning with sub-cycles was not computational efficiency but improved preservation of geometrical properties of the resulting skeleton. The erosion process implemented as a sequence of spatially oriented sub-cycles “peels” objects subsequently from different spatial directions and yields a better approximation of the center-line (spine) when compared to a sequential scan-oriented algorithm.

Considering the performances and the weaknesses of the different algorithms as discussed before the following thinning scheme was applied:

1. Pseudo-parallel thinning (using sub-cycles) to medial axis as proposed by Tsao and Fu [20]. Extending the concept of Tsao and Fu with sub-cycles in the six U,B,N,S,W,E directions we used 18 directions oriented along the c_{18} neighbor voxels. For each sub-cycle, connectivity is checked in the two 3×3 planes containing the active direction. The resulting skeleton is topologically correct but still contains some segments which are not maximally thinned.
2. Sequential thinning to achieve a maximal erosion of the skeleton to one voxel width. The algorithm is based on preservation of the genus χ_3 in $3 \times 3 \times 3$ voxel neighborhoods (see appendix equation 7). An additional check of the number of connected object components before and after deletion of the central voxel guarantees topology preservation. Line-ends are preserved by the condition that at least two object voxels must remain in each $3 \times 3 \times 3$ neighborhood.

The computation is not as easy as in the 2-D case, where the 256 possibilities can be prestored in a look-up-table for a highly efficient implementation. Object voxels are stored in list structures. Deletion of one voxel creates a new voxel appearing on the object surface which is appended to the list. At the same time, the neighborhood codes of the adjacent voxels are updated. The voxel-neighborhoods are represented with 26 bits in a 32 bit number; the three Δ 's (equation 7) are calculated with bit masks and bit operations. The test on the object components can be efficiently determined by calculating the number of 26-connected components 26-adjacent to the center voxel (\mathcal{C}), as proposed by Malandain et al. [22]. If $\mathcal{C} \neq 1$, the object would be split into several components with deletion of the center voxel.

The 3-D thinning scheme has been applied to the binary segmentation result of the cerebral vascular system obtained from MR angiography data (Figure 1b). The thinned structures are displayed using surface rendering (Figure 5a). It is obvious that the vessel structures are replaced by a reasonable approximation to its medial axes. The algorithm based on the preservation of the genus and the additional test for the number of components guarantee that the topology is preserved, which is an essential property not to break vessels into parts.

2.3 Estimation of object width by 3-D distance transform

For the complete geometrical description of the cerebral vessel tree, the midlines resulting from the thinning procedure have to be attributed with the local description of the cross section of the vessel. In the simplest case, if the vessels were approximated with circular cylinders, the cross section can be sufficiently described with the radius of the circle, i.e. the vessel width. As a consequence of the pseudo-parallel thinning algorithm the center-line voxels lie near to the ideal Euclidean skeleton. For this reason the Euclidean distance from the background

at the position of the center-line voxels serves as a reasonable approximation of the local vessel radius.

One way to determine the distance of any vessel voxel from the background is to perform a Euclidean distance transformation of the background. As a true Euclidean distance transform is computationally very expensive, very often the chamfer distance is used instead [24, 25], which can be calculated more efficiently. However, the chamfer distance is only a rough approximation of the Euclidean distance.

Danielsson [15] has proposed a sequential quasi-Euclidean distance transform for 2-D binary images. His algorithm is based on the fact, that the Euclidean distance can be efficiently propagated through connected passes of the regular neighborhood graph of the image raster. The algorithm processes the image pixels sequentially by scanline linearization, forcing this way a causality sequence onto them. The image is scanned from top right to bottom left in the first path, and reversely in the second. At every scan the neighbours of the current pixels lying in the past (according to the current scan direction) are checked for the nearest object point (in the Euclidean sense), which is then propagated to the current pixel if necessary. This way the algorithm needs only $o(n)$ operations, where n is the number of pixels in the complete image, making it reasonably fast.

Danielsson has shown that the algorithm will not provide the correct Euclidean distance in all cases. He and also Yamada[26] have performed a detailed analysis of the error produced by the algorithm, and shown that the error remains in the *subpixel range* which is in our case completely satisfactory (one should remember, that the midline runs through raster points, consequently its position has at least a subpixel error too).

We generalized the Danielsson algorithm to 3-D. As the complexity of the algorithm still remains $o(n)$, the distance transform can be calculated in a few minutes even for very large (256^3) data sets. While no detailed analysis has been made for the expected error in 3-D, we expect that the maximal distance error will not be larger as in the 2-D case, as the connectivity of a regular raster in 3-D is much higher than in 2-D.

2.4 Compilation of thinned objects to a graph structure

The abstraction of objects to line structures and the compilation into image graphs would enable a structural analysis by means of graph theory tools. Higher level image analysis, which assigns semantic meaning to image structures using model knowledge, becomes feasible through the selection of relevant image structures by *subgraphs labeling*. While retaining the approximate reconstructibility, the skeleton structure serves as a data structure which can be traced by traversing lines, nodes and branchings systematically. The skeleton represented by voxel lists is compiled to a graph structure by connecting segments of pixels to sequences and assigning them to edges, vertices, and faces of a graph data structure. The properties of the abstract description lead to simple arithmetic operations for the traversal of the graph structure.

The 2D compilation scheme based on the λ -graph concept [14] has been extended to the compilation of 3D voxel patterns. The experience with appropriate graph representations in 2D has clearly demonstrated its usefulness and has strongly encouraged the development of a similar concept in 3D space. Figure 3b illustrates the concept. A compilation of the voxel structure Fig. 3b 1 using only 6-connectivity would disconnect the structure into several parts (Fig. 3b 2), whereas 26-connectivity via faces, edges and corners would result in redundant connections (Fig. 3b 3). The λ -graph approach deletes edge-connections where a redundant face-connection exists and deletes corner-connections where a redundant edge-connection exists, resulting in a unique graph-description of the thinned structure. A λ -code at each voxel is calculated from the 26-bit neighborhood-code with bit operations. Using the λ -code information, the object structures are traversed and the codes compiled to lists.

The λ -graph allows the generation of a data structure representing points, lines, nodes and surfaces (Figure 3a). It is obvious that this representation is well suited for tree-like structures composed of line features, as it allows a simple traverse. Surfaces (bottom example Figure 3a) and volumes will require a different representation scheme, possibly based on their contours or surfaces, respectively.

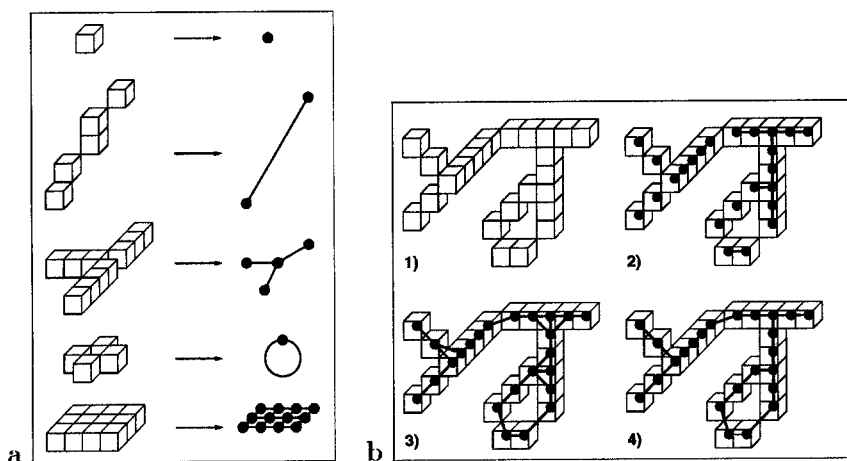


Figure 3: Object structures and their graph representation (a) and λ -graph (b): The c_6 - and c_{26} -graphs (2 and 3) of the original voxel structure (1) show either gaps or redundant connections. The λ -graph (4) represents a combination of the c_6 - and c_{26} -graphs and produces a unique connectivity.

Although correctly coded, certain configurations do not reflect the most favorable graph description. Figure 4 illustrates that optimally thinned corner configurations produce a face element in the graph description, which is topologically equivalent to a real hole (Fig. 4b). The detailed analysis of complex

configurations is a matter of future research. The problems can be approached by a high-level analysis of graph structures (e.g. by adding a missing edge voxel to the λ -graph) or by using voxel attributes from topological classification as proposed in [23] (the three voxels adjacent to the corner would be labeled as curve junctions).

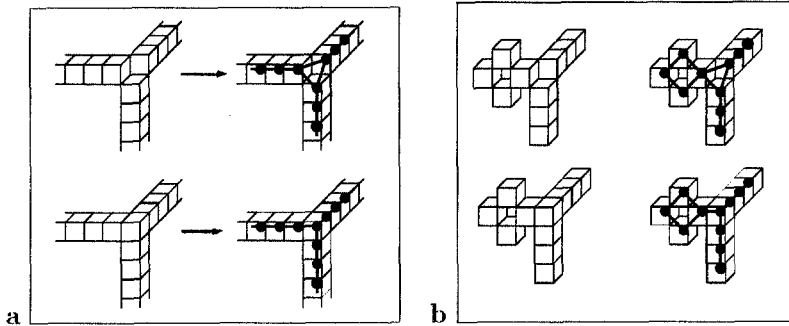


Figure 4: Sub-optimal coding of complex voxel configurations: Maximal thinning can counteract an optimal coding of curve junctions. The missing corner voxel (a and b top) creates a face element in the graph structure, which is topologically equivalent to the graph description of a hole (b bottom).

The output of the 3D thinning and compilation stages is a data structure containing both the topological description of the vessel tree and its geometric properties. It is implemented in an object-oriented design. Each of the different elements is represented by a class, these are :

- *Vessel Node* representing the branching and end points.
- *Vessel Link* representing the topological linkage between the *Nodes*
- *Vessel Point* holding all the geometric information available from the segmentation scheme such as local width, as well as additional attributes that can be computed (local direction, length, volume)
- *Vessel Trajectory* representing a sequence of points and as such the geometric path between *Nodes*

The *Vessel Tree* is implemented as a class containing lists of the above elements. Figure 5b represents a graphical visualization of the compiled vessel-tree. End nodes and branching nodes are displayed as spheres, whereas voxel-lists between nodes are represented as sequences of small tubes. It is then easy to formulate algorithms that travel the lists while fulfilling certain tasks. For example, we have implemented a filter-modul that removes “hair”-structures, i.e. short lines between end-nodes and branching nodes. The vessel tree can be reconstructed from the underlying data by traversing the trajectories and translating the geometric description in a format suitable for a renderer. By assigning

geometrical primitives to the symbolic elements of the graph structure, for example cylinders with radii equal to the width attribute, it is possible to visualize the symbolic description. (Figure 6).

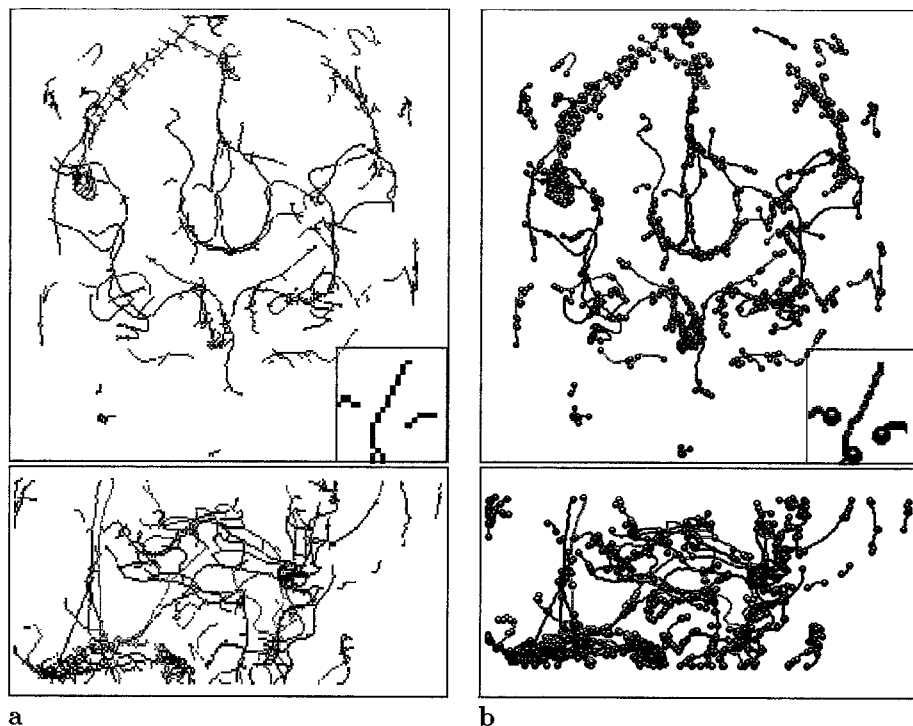


Figure 5: a) Result of 3-D binary thinning. The segmented vessel tree is maximally thinned to one voxel width by preserving topology and approximating center-lines. b) Graphical display of graph data structure describing the cerebral vessel-tree: End nodes and branching nodes are displayed as spheres, interconnecting vessel arcs as flexible pipes.

3 Results

The present paper discusses a prototype image analysis system that extracts and describes curvilinear structures from volume data.

A subgroup of medical image data is being composed of relatively homogeneous areas with high-contrast structures. This simplified world model allows a segmentation by thresholding, because the intensities of voxels are closely related to the structures of interest. Our tests with several 3-D MRA data sets demonstrated that segmentation by hysteresis thresholding was superior to sim-

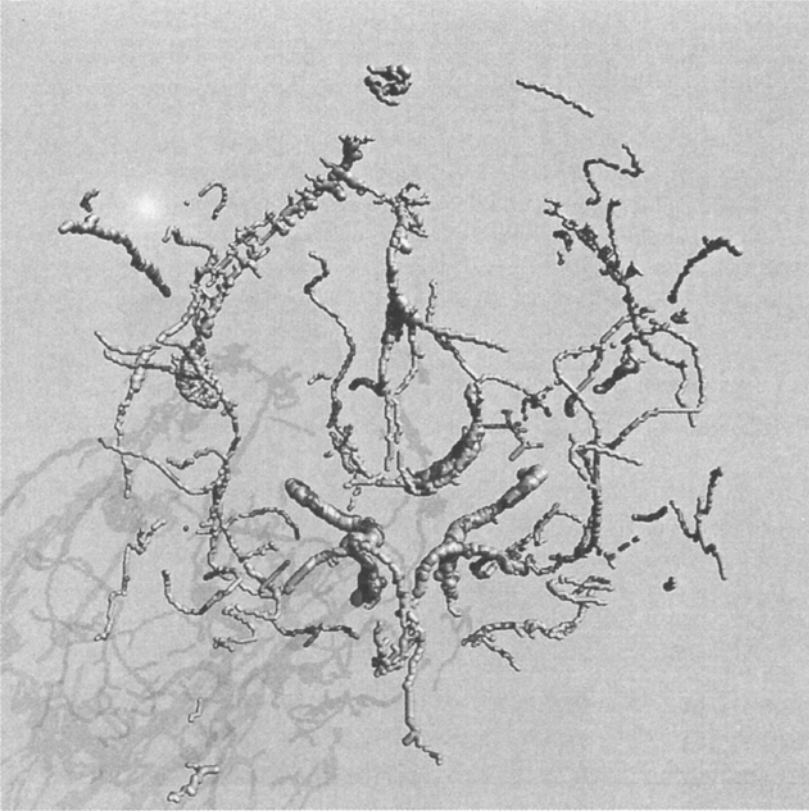


Figure 6: Three-dimensional rendering (ray-tracing) of structures encoded by the symbolic graph description. Vessel components are displayed as cylinders with radius estimated from the vessel width attribute. This display represents a kind of reconstruction which should come close to the rendering of the segmentation result, since the topology is preserved and local shape approximated by circular cylinders.

ple thresholding. We are well aware that this low-level segmentation of vessels from MRA is still insufficient, depicting only the largest vessels and creating gaps. These deficiencies are clearly visible as isolated vessel pieces (Figure 5), having only very limited anatomical meaning. Current developments investigate multiresolution matched filter techniques based on higher order directional derivatives of the Gaussian.

Binary thinning of tree-like structures to maximally thinned skeletons was still an open problem, as discussed in subsection 2.2. The preservation of topology has high priority as one wants to avoid creating gaps. The approximation of the center-line, however, is important too in order to generate a medial axis

description. The thinning scheme presented here combines a pseudo-parallel algorithm proposed by Tsao and Fu [20] (extended to more sub-cycles) with a sequential algorithm based on the constancy of the 3-D genus and an additional check of the number of object components. Careful tests on highly complex structures proved that the topology is preserved while object structures are thinned to voxel lists. The latter is a necessary property with regard to a raster-to-vector transformation.

The compilation method represents a 3-D extension of the 2-D λ -graph concept. The thinned structures in the 3-D volume array are transformed into a graph description. Vessel segments are represented as lists of vectors which can additionally be attributed with geometric features. Assuming a maximally thinned object as input, the compilation method poses no algorithmic and technical problems. It is illustrated in Figure 3a that the proposed data structure is well suited to represent tree-like object structures. Surfaces obtained by 3-D edge detection or medial surfaces, however, will require a different data structure taking into account the sheet elements. Further, some complex configurations (Figure 4) still need an improved graph description.

One of the important local features of a vessel tree is the vessel diameter. An estimation of the local width is obtained by a 3-D Euclidean distance transform applied to the binary segmentation result. Each voxel gets a label expressing its distance to the nearest boundary. Although the location of the skeleton obtained by thinning does not always match the ideal center-line, the width estimation can serve as an initial guess when smoothed along vessel components.

4 Outlook

The final output of the 3-D thinning and compilation stages is a data structure representing voxel-lists, branchings and approximate local diameter. This symbolic representation codes the geometry and the topology information of the vessel tree. A further advantage of the object-centered description is its invariance (up to an error introduced by the pseudo-parallel thinning) with respect to standard transformations, i.e. translation and rotation, and even to nonlinear distortions.

The methods developed in this project could be useful in application areas where not only a display of blood vessels, but *structural information* about their spatial extension and the relationship among vascular components and to anatomical objects is required.

Neuroradiological diagnosis could be improved by new tools for the analysis of 3-D MRA data. Stereotactic neurosurgery needs knowledge about the relative position of major vessels to the structure to be treated, for example a tumor. Changes on the vascularity are a significant aspect of the clinical evaluation of a tumor, as vessels can be displaced, incorporated or even newly formed. A combined display of the segmented vascular structure with soft tissue and trajectories of instruments would allow surgical planning to avoid perforating major arteries. Besides a visual assessment of the vascularity, malformations or criti-

cal changes could be expressed by a comparison of the symbolic representation with appropriate neuroanatomical models (anatomical atlas). The study of the cerebro-vascular topology would provide not only the information *that* a blood vessel is found at a specific location but also *how* a vessel component is connected to its predecessors and successors.

Multimodality analysis of image data from different scanners becomes increasingly important. A symbolic description of the 3-D vessel tree can provide point-landmarks (e.g. at branching locations) to perform a registration of 3-D MRA with 2-D DSA (Digital Subtraction Angiography) projections. Specific properties of both, the 3-D mapping provided by MRA and the high resolution offered by DSA, could be combined either to correct MRA data for distortions and artifacts or to perform graphical display of details of the vessels only obtained with DSA.

In interventional radiology procedures, blood vessels could be damaged during the implementation of endo-vascular catheters. The information about the vascular topology would be helpful guiding endo-vascular instruments. The structural description of the cerebral vessel tree will offer a systematic traversal based on topological and geometrical criteria.

The discussion of potential applications indicates that a successful segmentation and description of the vessel tree could represent an important new tool for clinical diagnosis, planning and treatment. Two issues will be considered in future developments, an improved segmentation that extracts vessels down to one voxel diameter and the implementation of graph-analysis tools for structural interpretation and model-based analysis.

Appendix: Genus in 3-D Space

The net contribution of a voxel to the global connectivity number of a 3-D structure can be determined by a relation based on a combination of the globally defined *genus* (eq. 2) with geometric constraints imposed on a structure given by the *Euler-Schlaefli formula* (eq. 3 for structures which need not be simply connected):

$$\chi_3(S) = \text{Objects}(S) + \text{Cavities}(S) - \text{Holes}(S) \quad (2)$$

$$v(G) - e(G) + f(G) - q(G) = -h(G) \quad (3)$$

$$v(G) - e(G) + f(G) - u(G) = \text{Objects}(G) + \text{Cavities}(G) - \text{Holes}(G) \quad (4)$$

where v, e, f and q define the number of vertices, edges, faces and cells (including elementary cells u , cavities and background cell: $q(G) = u(G) + \text{Cavities}(G) + 1$) of a 3-D singly connected structure G . Structures dealt with are not necessarily singly connected, requiring the definition of a new structural element h ("hole" or "handle"). The number of holes h is defined as the amount by which the sum differs from zero (eq. 3). As pointed out by Morgenthaler [21], the concept of 3-D holes is different from objects and cavities since we cannot

label points which constitute a hole to facilitate counting them. Equation 3 is summed over every component O of an image to obtain the final relation 4. Considering that objects S define cavities in the complement \bar{S} and vice-versa (with correction for the background component), equations 2 and 4 are combined to express the genus $\chi_3(S)$ of a 3-D structure in terms of elements constituting the graph structure.

$$\begin{aligned}\chi_3(S) &= \text{Objects}(S) + \text{Cavities}(S) - \text{Holes}(S) \\ &= \text{Cavities}(\bar{S}) + (\text{Objects}(\bar{S}) - 1) - \text{Holes}(\bar{S}) \\ &= v(\bar{S}) - e(\bar{S}) + f(\bar{S}) - u(\bar{S})\end{aligned}\quad (5)$$

Most often, image objects S are chosen to be 26-connected (c_{26}) and embedded in a 6-connected (c_6) background \bar{S} . Vertices, edges, faces and cells of the graph $c_6(\bar{S})$ can be measured locally and summed up for computing the three-dimensional genus.

Thinking about topology-preserving thinning, the removal of a voxel s from a set S should not change the genus χ_3 :

$$\chi_3(S) - \chi_3(S \setminus s) \equiv 0 \quad (6)$$

$$\Delta v(\bar{S}) - \Delta e(\bar{S}) + \Delta f(\bar{S}) - \Delta u(\bar{S}) \equiv 0$$

$$\text{voxel deletable if: } \Delta e(\bar{S}) - \Delta f(\bar{S}) + \Delta u(\bar{S}) \equiv 1. \quad (7)$$

The contributions Δv , Δe , Δf and Δu can be calculated in local $3 \times 3 \times 3$ voxel neighborhoods. With Δv becoming 1, the condition leading to a decision at each voxel can be simply defined as shown in eq. 7. The equation describes the change of elements in the graph of a voxel structure with connectivity c_6 if the central voxel of a $3 \times 3 \times 3$ neighborhood is deleted. The condition assures that the genus χ_3 will be preserved. However, as explained in the text, the topology of structures will not necessarily be kept.

Acknowledgements

Part of this research work was funded by COVIRA (Computer Vision in Radiology), project A2003 of the AIM (Advanced Informatics in Medicine) programme of the European Commission.

Participants in the COVIRA consortium are:

Philips Medical Systems, Best (NL) and Madrid (E), Corporate Research, Hamburg (D) (prime contractor); Siemens AG, Erlangen (D) and Munich (D); IBM UK Scientific Centre, Winchester (UK); Gregorio Maranon General Hospital, Madrid (E); University of Tübingen, Neuroradiology and Theoretical Astrophysics (D); German Cancer Research Centre, Heidelberg (D); University of Leuven, Neurosurgery, Radiology and Electrical Engineering (B); University of Utrecht, Neurosurgery and Computer Vision (NL); Royal Marsden Hospital/Institute of Cancer Research, Sutton (UK); National Hospital for Neurology and Neurosurgery, London (UK); Foundation of Research and

Technology, Crete (GR); University of Sheffield (UK); University of Genoa (I); University of Aachen (D); University of Hamburg (D); Swiss Federal Institute of Technology, Zurich (CH)

The MRA data were provided by Siemens AG, Erlangen, Germany and by Dr. F. Jolesz, Brigham and Women's Hospital, Boston, USA.

References

- [1] H-H. Ehrlicke and G. Laub. Combined 3D-display of cerebral vasculature and neuroanatomic structures in mri. In K.H. Höhne, H. Fuchs, and S.M. Pizer, editors, *3D Imaging in Medicine*, pages 229–239, Berlin Heidelberg, June 1990. Springer-Verlag.
- [2] K.H. Höhne, M. Bomans, A. Pommert, M. Riemer, et al. Rendering tomographic volume data: Adequacy of methods for different modalities and organs. In K.H. Höhne, H. Fuchs, and S.M. Pizer, editors, *3D Imaging in Medicine*, pages 197–215, Berlin Heidelberg, 1990. Springer-Verlag.
- [3] D. Vandermeulen, D. Delaere, P. Suetens, H. Bosmans, and G. Marchal. Local filtering and global optimisation methods for 3d magnetic resonance angiography (mra). In Richard A. Robb, editor, *Visualization in Biomedical Computing*, pages 274–288. SPIE, October 1992.
- [4] Society of Magnetic Resonance in Medicine, SMRM. *Proceedings of SMRM conference held at San Francisco*, August 1991. abstracts 210, 757, 820, 1229.
- [5] H-H. Ehrlicke, L.R. Schad, G. Gademann, B. Wowra, et al. Use of MR angiography for stereotactic planning. *Journal of Computer Assisted Tomography*, 16(1):35–40, January 1992.
- [6] H.E. Cline et al. Vascular morphology by three-dimensional magnetic resonance imaging. *Mag. Res. Im., Pergamon Press*, 7:45–54, 1989.
- [7] D.N. Levin et al. The brain: integrated three-dimensional display of MR and PET images. *Radiology*, 17:783–789, 1989.
- [8] H. Blum. A transformation for extracting new descriptors of shape. In E. Dunn, W., editor, *Models for the Perception of Speech and Visual Form*, Cambridge, MA, 1967. M.I.T. Press.
- [9] J. Niggemann. Analysis and representation of neuroanatomical knowledge. *Applied Artificial Intelligence*, 4:309–336, 1990.
- [10] J.F. Canny. Finding edges and lines in images. Technical Report 720, MIT Artificial Intelligence Laboratory, Dept. of Electrical Engineering and Computer Science, Cambridge, MA, 1983.
- [11] J.F. Canny. A computational approach to edge detection. *IEEE Transactions on Pattern Analysis and Machine Intelligence*, 8(6):679–698, 1986.
- [12] O. Monga et al. Recursive filtering and edge closing: two primary tools for 3D edge detection. In O. Faugeras, editor, *Proc. First European Conference on Computer Vision - ECCV'90*, pages 56–65, Berlin-Heidelberg, May 1990. Springer-Verlag.
- [13] C. Arcelli and B. Sanniti di Baja. A width-independent fast thinning algorithm. *IEEE Transactions on Pattern Analysis and Machine Intelligence*, 7(4):463–474, 1985.

- [14] P.T. Speck. *Übersetzung von Linien und Flächenstrukturen in kombinatorisch-relationale Datenstrukturen zur automatischen Mustererkennung in Digitalbildern*. PhD thesis, ETH Zurich, 1984. Ph.D. thesis No. 7508.
- [15] P.E. Danielson. Euclidean distance mapping. *Computer Graphics and Image Processing*, 14:227–248, 1980.
- [16] L. Dorst. Pseudo-euclidean skeletons. In *Proc. 8. ICPR, Paris*, pages 286–288, 1985.
- [17] D.G. Morgenthaler. Three-dimensional simple points: serial erosion, parallel thinning, and skeletonization. Technical Report TR-1005, Computer Vision Laboratory, University of Maryland, College Park, MD 20742, USA, February 1981.
- [18] T.Y. Kong and A. Rosenfeld. Digital topology: Introduction and survey. *Computer Vision, Graphics, and Image Processing*, 48:357–393, 1989.
- [19] S. Lobregt, P.W. Verbeek, and F.C.A. Groen. Three-dimensional skeletonization, principle and algorithm. *IEEE Transactions on Pattern Analysis and Machine Intelligence*, 2(1):75–77, January 1980.
- [20] Y.F. Tsao and K.S. Fu. A parallel thinning algorithm for 3-D pictures. *Computer Graphics and Image Processing*, 17:315–331, 1981.
- [21] D.G. Morgenthaler. Three-dimensional digital topology: The genus. Technical Report TR-980, Computer Vision Laboratory, University of Maryland, College Park, MD 20742, USA, November 1980.
- [22] G. Malandain, G. Bertrand, and N. Ayache. Topological classification in digital space. In A.C.F. Colchester and D.J. Hawkes, editors, *Information Processing in Medical Imaging, IPMI'91*, pages 300–313, Berlin-Heidelberg, 1991. Springer-Verlag.
- [23] G. Bertrand and G. Malandain. A new topological classification of points in 3d images. In G. Sandini, editor, *Computer Vision - ECCV'92*, pages 710–714, Berlin Heidelberg, 1992. Springer-Verlag.
- [24] G.T. Herman and C.A. Bucholtz. Shape-based interpolation using a chamfer distance. In *Proceedings of IPMI'91, Wye*, pages 314–325. Springer-Verlag, 1991.
- [25] K.J. Zuiderveld, A.H. Konong, and M.A. Viergever. Acceleration of ray-casting using 3-d distance transforms. In *Proceedings of VBC'92, Chapel Hill*, pages 336–346. SPIE Conf. Ser. Vol. 1808, 1992.
- [26] H. Yamada. Complete euclidean distance transformation by parallel operation. In *Proc. 7th ICPR*, pages 69–71, 1984.